Int. J. Heat Mass Transfer. Vol. 17, pp. 61–67. Pergamon Press 1974. Printed in Great Britain

ANALYSIS OF THE EFFECTS OF VAPOR PRESSURE DROP ON HEAT PIPE PERFORMANCE

C. L. TIEN and A. R. ROHANI
Department of Mechanical Engineering, University of California, Berkeley, California 94720, U.S.A.

(*Received* 5 *April* 1973 *and in revised form* 18 *June* 1973)

Abstract—An analysis of the effects of vapor pressure variation on the vapor temperature distribution, evaporation and condensation rates, and the overall heat pipe performance is presented. The elliptic mass, momentum and energy conservation equations in conjunction with the thermodynamic equilibrium relation and appropriate boundary conditions are solved numerically for a cylindrical heat pipe with evaporator, adiabatic and condenser sections. The results show that in certain situations vapor pressure variations play a significant role in the heat pipe performance. It is also demonstrated that the approximate solution based on the parabolic boundary-layer equations does not provide an accurate picture of vapor pressure variations at relatively high evaporation and condensation rates.

NOMENCLATURE

c_p, specific heat at constant pressure;
h, enthalpy, $c_p T$;
h_{fg}, heat of vaporization;
H, overall heat transfer coefficient;
L, length of the heat pipe,
p, pressure;
P, perimeter;
Q, overall heat transfer rate through the heat pipe;
r, radial distance;
r_0, vapor space radius;
Re, radial Reynolds number, $\rho r_0 v_0/\mu$;
T, temperature;
T_0, initial operating vapor temperature;
u, axial velocity;
v, radial velocity;
v_0, evaporation or condensation velocity;
x, axial distance;
Γ_h, thermal exchange coefficent;
μ, viscosity;
ρ, density;
ψ, stream function;
ω, vorticity.

Subscripts

a, ambient;
c, condenser;
e, evaporator;
s, value on the boundary.

1. INTRODUCTION

ALONG the vapor–liquid interface inside a heat pipe the vapor temperature is related to the pressure according to the equlibrium temperature–pressure relation. Therefore, a large pressure drop in the vapor-flow direction may result in a significant temperature drop along the interface, thus affecting the overall heat pipe performance. The pressure-drop effect becomes more pronounced in a long heat pipe or in cases where the operating vapor pressure is relatively small, such as in liquid metal heat pipes. There have been several recent investigations [1–4] to analyse the effects of vapor flow, particularly the effect of pressure variations, on the overall heat pipe performance. These analyses were all based on mass and momentum conservation equations and thus neglected the complex coupling with the energy equation and the thermodynamic equilibrium relation. Moreover, the boundary-layer approximation was often employed [1, 2, 4] in a problem clearly of elliptic type, and the validity of this approximation in the case with appreciable vapor pressure drop has not been assessed.

In the present paper the effects of vapor pressure variation on the axial temperature distribution, evaporation and condensation rates, and the overall heat pipe performance are investigated analytically. The theoretical framework is based on the elliptic mass, momentum and energy conservation equations as well as the thermodynamic equilibrium relations. Results are obtained numerically for a cylindrical heat pipe with evaporator, adiabatic, and condenser sections. Several cases of heat pipe operation with significant vapor pressure drop are considered. The present findings are in general agreement with the temperature measurements of Busse [4] on a liquid metal heat pipe, and with the earlier approximate calculations. The effects of radial pressure drop are

also indicated by comparing with the boundary layer calculations in which the radial pressure gradient is neglected.

2. FUNDAMENTAL EQUATIONS

The physical model under consideration is a cylindrical heat pipe with evaporator, adiabatic and condenser sections, operating under the following assumptions:

1. The steady flow of vapor is laminar and subsonic.
2. The vapor has constant transport properties and its density variations follow the prefect-gas law.
3. At the vapor–liquid interface, the vapor is at its equilibrium temperature corresponding to its pressure. Elsewhere it is either superheated or subcooled depending on the local temperature and pressure. Evaporation and condensation take place only at the vapor–liquid interface.
4. The evaporator and condenser are surrounded by constant but different ambient temperatures and are associated with uniform overall heat transfer coefficients between the vapor–liquid interface and the ambient. This assumption will have a magnifying effect in demonstrating the effects of axial pressure variations and consequent temperature distribution along the vapor–liquid interface on the heat pipe performance. In actual situations, the heat transfer coefficient between the heat pipe and its ambient is a complex function of the ambient and heat pipe wall temperature, the dominant mode of heat transfer and the material of the heat pipe wall and liquid wick matrix as well as other parameters.
5. The effects of axial heat conduction through the pipe wall and liquid wick matrix as well as the liquid pressure drop in the wick are negligible. This assumption is rather restrictive for many heat pipes [5] and is imposed here primarily for the purpose of focusing our attention on the complex transport phenomena in the vapor region. The present numerical framework, however, could incorporate these effects [5] in a more extensive computational study.

Enclosure relations

The heat pipe is a closed system such that at steady state the mass of the vapor generated and the energy transferred into the system in the evaporator section must be equal to the mass of the vapor condensed and the energy rejected out of the condenser section, respectively. The energy enclosure condition gives

$$Q \equiv \int_{L_e} H_e P[T_{ae} - T_0(x)]\,dx = \int_{L_c} H_c P[T_0(x) - T_{ac}]\,dx \qquad (1)$$

where all symbols are defined in Nomenclature. For given values of H_e, T_{ae}, H_c and T_{ac}, $T_0(x)$ must assume such an expression that the above integral conservation relation as well as the following differential conservation equations are satisfied.

Governing differential equations

For the numerical method of analysis [5] employed in the study, it is more convenient to express the mass, momentum and energy conservation equations in terms of stream function, vorticity and enthalpy:

$$\frac{\partial}{\partial x}\left[\frac{1}{\rho r}\left(\frac{\partial \psi}{\partial x}\right)\right] + \frac{\partial}{\partial r}\left[\frac{1}{\rho r}\left(\frac{\partial \psi}{\partial r}\right)\right] + \omega = 0 \qquad (2)$$

$$r^2\left[\frac{\partial}{\partial x}\left(\frac{\omega}{r}\frac{\partial \psi}{\partial r}\right) - \frac{\partial}{\partial r}\left(\frac{\omega}{r}\frac{\partial \psi}{\partial x}\right)\right] - \frac{\partial}{\partial x}\left[r^3\frac{\partial}{\partial x}\left(\mu\frac{\omega}{r}\right)\right] - \frac{\partial}{\partial r}\left[r^3\frac{\partial}{\partial r}\left(\mu\frac{\omega}{r}\right)\right] = 0 \qquad (3)$$

$$\left[\frac{\partial}{\partial x}\left(h\frac{\partial \psi}{\partial r}\right) - \frac{\partial}{\partial r}\left(h\frac{\partial \psi}{\partial x}\right)\right] - \frac{\partial}{\partial x}\left[\Gamma_h r\frac{\partial h}{\partial x}\right] - \frac{\partial}{\partial r}\left[\Gamma_h r\frac{\partial h}{\partial r}\right] = 0 \qquad (4)$$

where

$$\frac{\partial \psi}{\partial r} = \rho u r, \quad \frac{\partial \psi}{\partial x} = -\rho v r$$

and

$$\omega = \frac{\partial v}{\partial x} - \frac{\partial u}{\partial r}. \qquad (5)$$

Boundary conditions

Boundary conditions for the above equations are specified in accordance with the requirements for the boundary conditions of the elliptic differential equations. For heat pipe vapor space, in order to determine the stream function, vorticity and temperature boundary conditions, pressure distribution in the system must be first prescribed. Initially, a uniform pressure is selected by assuming the vapor at a constant temperature T_0 calculated from equation (1)

$$T_0 = \frac{\int_{L_e} HPT_a\,dx}{\int_{L_c} HP\,dx} \qquad (6)$$

based on the vapor–liquid equilibrium relation. The magnitude of pressure is adjusted during the calculation procedure by a successive approximation procedure in such a way that the system always satisfies the energy balance relation.

Once a value of the pressure inside the heat pipe is designated, the temperature boundary condition on

the pipe wall is obtained from the vapor–liquid equilibrium relation

$$T = T(p) \tag{7}$$

where the complicated T–p relationship will be approximated with a linear relation at points close to the operating pressure of the system. The minor deviations in temperature values due to this approximation would have a minimal effect on the outcome of the analysis. Other boundary conditions are at the insulated heat pipe flat ends:

$$\left.\frac{\partial T}{\partial x}\right|_{x=0,\,L} = 0 \tag{8}$$

and at the pipe centerline

$$\left.\frac{\partial T}{\partial r}\right|_{r=0} = 0. \tag{9}$$

The velocity components u and v at the boundary must satisfy:

$$v(0, r) = v(L, r) = v(x, 0) = 0,$$

$$u(0, r) = u(L, r) = u(x, r_0) = 0, \quad \left.\frac{\partial u}{\partial r}\right|_{r=0} = 0. \tag{10}$$

The evaporation and condensation velocity, v_0, is determined by writing the energy balance relation for an axial element of the vapor–liquid interface and by

$$v_0(r_0, x) = \left[H(T_0(x) - T_a) + k\left.\frac{\partial T}{\partial r}\right|_{r_0}\right]/[\rho h_{fg}]. \tag{11}$$

The stream function, ψ, on the boundary is determined by integrating equations (5),

$$\begin{aligned} &\psi(0, r) = \psi(L, r) = \psi(x, 0) = 0 \\ &\psi(x, r_0) = -\int_0^x \rho v_0 r_0 \, dx. \end{aligned} \tag{12}$$

Vorticity boundary conditions at the vapor–liquid interface and on the heat pipe flat ends are calculated by assuming that the vorticity is uniform close to the boundary [3, 6]

$$\omega_s = -\frac{(\psi_1 - \psi_s)}{r_s n_1 \rho} \tag{13}$$

and a relation based on the assumption that vorticity variations close to centerline are parabolic was used for determination of ω/r on the pipe axis.

3. SOLUTION PROCEDURE

Basically, the finite difference iterative method of solution with the upwind method of differencing of Gosman *et al.* [6] was employed in the present analysis. In brief, the field under study is divided into M rows and N columns, and row and column numbers are assigned to the nodes of the grid that is formed. Then, the three conservation equations are written in algebraic difference form by using the upwind method. Three sets of MN difference equations in the general form of

$$\phi_{i,j} = C_{i+1,j}\phi_{i+1,j} + C_{i-1,j}\phi_{i-1,j} + C_{i,j+1}\phi_{i,j+1} + C_{i,j-1}\phi_{i,j-1} + D_{ij} \tag{14}$$

are obtained for the three differential conservation equations. The Gauss–Seidel point iterative method is used to solve the 3 MN algebraic equation.

The solution procedure for the simple heat pipe system is in the following order:

1. Zero initial values of stream function and vorticity are assumed for nodes inside the grid. Vapor temperature is assumed constant and equal to T_0 from equation (6) at all nodes of the grid.

2. Velocity and stream function boundary conditions are determined from equations (10)–(12), and the set of difference equations for stream function is solved.

3. With the new stream function values, vorticity boundary conditions are determined, and the set of difference equations for vorticity is solved.

4. From the new stream function values, velocity components are calculated from equation (4) for nodes inside the grid. By knowing the velocity field, the pressure distribution along the vapor–liquid interface is determined by integration of the momentum equation (6). Pressure at the liquid–vapor interface at the end of evaporator section, p_0, is taken as the datum pressure and does not change. With the new pressure distribution, the temperature boundary condition is determined from equations (7)–(9), and the set of difference equations for temperature is solved.

5. Steps 2–4 are repeated, and in each subcycle of iteration the maximum value of R_ϕ, as defined below, is calculated

$$R_\phi = 1 - \frac{\phi^{N+1}}{\phi^N}. \tag{15}$$

The procedure is terminated when R_ϕ becomes less than a small preassigned value (here taken as 0·001) for all the dependent variables ω, ψ and h.

The initial uniform distribution of $T_0(x)$ is modified in the course of calculation. In order to satisfy the energy enclosure relation, equation (1), the average value of temperature at the vapor–liquid interface defined as

$$T_{av} = \left[\int_L HPT_0(x)\,dx\right]/\left[\int_L HP\,dx\right] \tag{16}$$

must be equal to T_0 from equation (6). This is made possible by calculating the pressure p_{av} related to T_{av} from equation (7). Subtracting this pressure from the datum pressure p_0^N and adding the results of subtraction to p_0^N would constitute the new datum pressure p_0^{N+1}. In the course of obtaining the results this adjustment was made only after every N steps of iteration. Also, the vapor density variation is taken into consideration in this sequence.

4. RESULTS AND DISCUSSION

A cylindrical heat pipe with sodium as working fluid was selected for the analysis. The pipe dimensions were chosen close to the dimensions of an experimental heat pipe operating in Berkeley (i.e. $L = 0{\cdot}6$ m, $L_e = 0{\cdot}2$ m, $L_c = 0{\cdot}3$ m and $r = 0{\cdot}0086$ m). The range of heat pipe operating temperature that was studied is such that while the operating pressure inside the system is low, the pressure drop along the pipe is relatively large. The heat pipe evaporator and condenser ambient temperatures and overall heat transfer coefficients were assumed constant. Thus, by neglecting the vapor temperature variations due to its pressure drop, evaporation and condensation rates must be uniform. Five cases of heat pipe operation with various evaporation and condensation rates were studied. This range was selected in such a way that the maximum vapor Reynolds number, based on the average axial velocity in the adiabatic section and pipe diameter, did not exceed the limit beyond which turbulent flow might occur. This limiting Reynolds number was taken as 2100 while occasionally laminar flows of much higher Reynolds numbers are encountered. Table 1 gives the primary information on these cases. A 61 × 10 grid was used for obtaining the results of the above-mentioned cases. The computer time spent on CDC 6400 was about 2 min for each case, and the density and pressure correction was made after every 10 steps of iteration.

In presenting the results, flow aspects of the problem have been omitted because of its similarity to the results reported by Bankston and Smith [3]. Figure 2 demonstrates the vapor pressure drop along the heat pipe vapor–liquid interface for the Runs No. 1–5 in Table 1. The pressure drop profile in the adiabatic section is a straight line similar to Poiseuille flow results, while profiles in the evaporator and condenser sections demonstrate the effects of the pressure head absorbed or created by evaporation or condensation. The overall pressure drop along the heat pipe in all cases is very close to predictions of Busse [1] and Cotter [2] for low evaporation and condensation rates on the basis of Poiseuille flow relationships. For the present cases, the results on the basis of Poiseuille flow equations are obtained by extending the almost uniform pressure drop line in the adiabatic section from both sides to the middle points of evaporator and condenser sections. The effect of this vapor pressure drop on temperature variations along the heat pipe vapor–liquid interface is demonstrated in Fig. 3. The profiles are obtained from the vapor–liquid equilibrium relations for

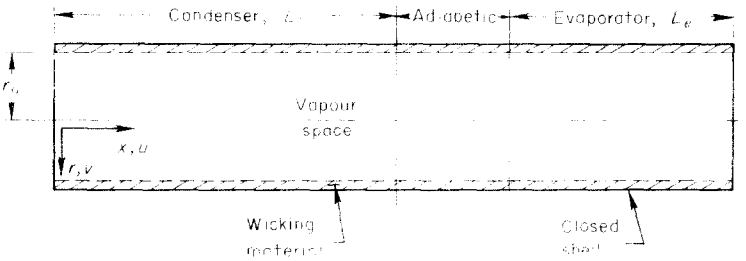

FIG. 1. Schematic diagram of the heat pipe.

Table 1. Primary information on the sodium liquid metal heat pipe

Run no.	T_{ac} (K)	T_{ae} (K)	H_c (W m^{-2} K^{-1})	H_e (W m^{-2} K^{-1})	Re_e	Re_c	T_0 (K)	p_0 (N/m^2)
1	800	805	17106	2851	2	1·33	804	946
2	800	810	17106	2851	4	2·66	808	1023
3	800	820	17106	2851	8	5·33	816	1203
4	800	830	17106	2851	24	16·00	824	1398
5	800	845	17106	2851	36	24·00	836	1633

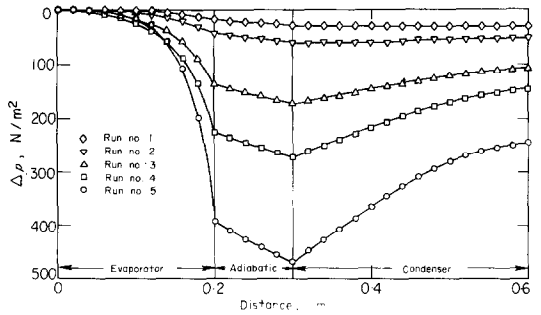

FIG. 2. Axial wall pressure drop along the heat pipe.

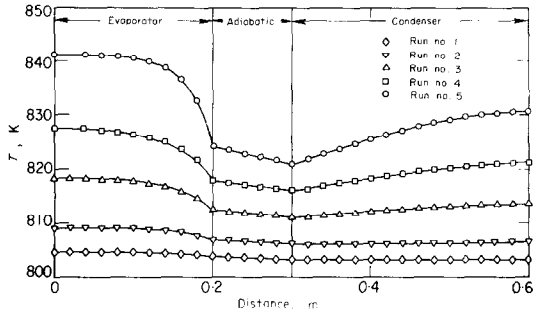

FIG. 3. Axial wall temperature drop along the heat pipe.

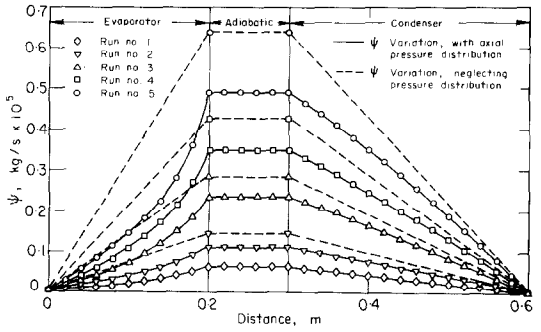

FIG. 4. Distribution of stream function on the heat pipe wall.

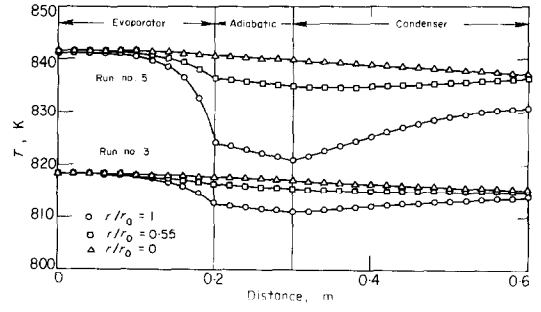

FIG. 5. Axial temperature variation at various radial locations.

sodium. The temperature distribution in each case is compared with the uniform temperature T_0 when the effects of the vapor pressure drop are neglected. A temperature drop of about 20°K is resulted in Run No. 5. The temperature recovery in condenser section in Runs No. 2–5 has also been observed in the experimental measurements by Busse [4] of a liquid metal heat pipe.

The effects of the temperature variation along the heat pipe on its performance is demonstrated in Fig. 5 where the actual stream function variation along the heat pipe vapor–liquid interface is compared with the values expected when the effect of the vapor pressure drop is neglected. Because of the temperature drop, the maximum value of the stream function in the adiabatic section is lower than the expected uniform value in all cases. The results of this reduction in the maximum value of stream function is a reduction in the overall heat transfer rate through the heat pipe as demonstrated in Table 2.

Table 2. Comparison of the actual and expected values of Q and Re_{max}

Run no.	Q_n (W)	$Re_{max,\,n}$	Q (W)	Re_{max}
1	185	186	162	163
2	370	372	289	292
3	740	744	610	614
4	1120	1126	906	911
5	1665	1674	1265	1283

Considering the axial temperature variations at the vapor–liquid interface as shown in Fig. 3, the elliptic energy conservation equation was solved simultaneously with the stream function and vorticity equations by following the solution procedure already described. Figure 5 presents the axial temperature variations at various radial locations for Runs No. 3 and 5, while Figs. 6 and 7 show the radial temperature profiles at various axial locations for the same cases. These variations become important when the amount of heat that is transferred by conduction between liquid and vapor becomes significant. Bankston and Smith [3] reported the axial velocity reversals close to the vapor–liquid interface at the end of condenser section for high evaporation and condensation rates. The flow reversal exists also in the present cases with non-uniform evaporation and condensation. The effect of this reversal on radial temperature variations can be seen by a comparison of temperature profiles close to the vapor–liquid interface in Runs No. 3 and 5 (Figs. 6 and 7).

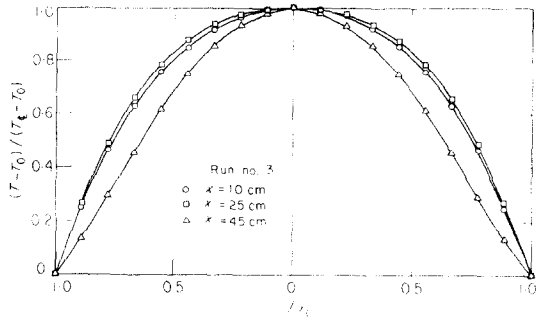

FIG. 6. Radial temperature variation at various axial locations.

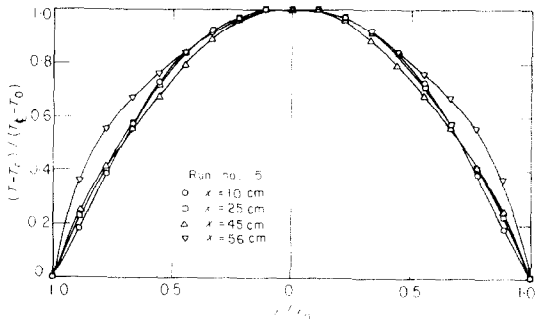

FIG. 7. Radial temperature variation at various axial locations.

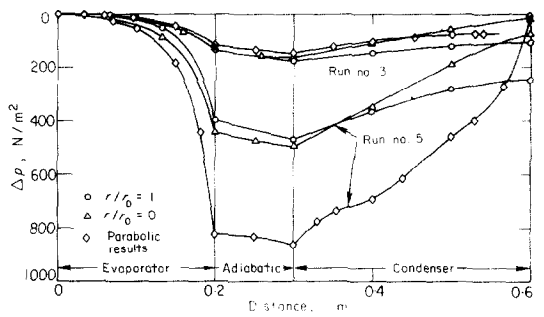

FIG. 8. Comparison of the elliptic and parabolic pressure drop results.

The momentum and energy conservation equations of the boundary layer type were also solved for the problem of vapor flow by following the numerical solution method of Spalding and Patankar [7]. A successive approximation method was used for calculation of axial pressure drop along the heat pipe and the same method of the elliptic case was applied for correction of the starting pressure at the heat pipe evaporator end. The pressure drop results obtained from the solution of the two sets of parabolic and elliptic equations for Runs No. 3 and 5 are compared in Fig. 8. For the elliptic results, pressure drop is calculated by integration of the momentum equation and having the velocity profiles from the solution of stream function and vorticity equations. On the other hand for the parabolic results, at each section along the pipe, a uniform pressure drop is first calculated being mainly a function of the rate of condensation. This uniform pressure drop is then used for calculation of the velocity profile at that section from the parabolic momentum equation. If this velocity profile does not satisfy the continuity equation, a new pressure drop term is selected and a successive approximation procedure is followed so that a uniform pressure drop is finally calculated which yields a velocity profile that satisfies the continuity equation. Considering the radial variations of pressure at the heat pipe condenser end as demonstrated in Fig. 8 from the results of elliptic equations, one cannot expect to obtain accurate results for velocity profile or axial pressure drop by using the same dp/dx at all radial location in a section along the heat pipe. At higher evaporation and condensation rates the boundary layer equations result in velocity and temperature profiles that have several maximum and minimum points and unstable pressure drop profiles, Run No. 5.

REFERENCES

1. T. P. Cotter, Theory of heat pipes, Los Alamos Scientific Laboratory, LA-3246-MS, (1965).
2. C. A. Busse, Pressure drop in the vapor phase of long heat pipes, Proceedings of the 1967 IEEE Thermionic Conversion Specialist Conference, Palo Alto, California, p. 391 (1967).
3. C. A. Bankston and H. J. Smith, Incompressible laminar vapor flow in cylindrical heat pipes, ASME Paper No. 71-WA/HT-15 (1971).
4. C. A. Busse, Theory of the ultimate heat transfer limit of cylindrical heat pipes, *Int. J. Heat Mass Transfer* **16**, 169–186 (1973).
5. A. R. Rohani and C. L. Tien, Steady two-dimensional heat and mass transfer in the vapor–gas region of a gas-loaded heat pipe, ASME Paper No. 72-WA/HT-34 (1972). To appear in *J. Heat Transfer*.
6. A. D. Gosman, W. M. Pun, A. K. Runchal, D. B. Spalding and M. Wolfstein, *Heat and Mass Transfer in Recirculating Flows*. Academic Press, New York (1969).
7. D. B. Spalding and S. V. Patankar, *Heat and Mass Transfer in Boundary Layers*. Morgan-Grampian, London (1967).

ANALYSE DES EFFETS DE LA CHUTE DE PRESSION DE VAPEUR SUR LES PERFORMANCES D'UN CALODUC

Résumé—On présente une analyse des effets de la variation de pression de vapeur sur la distribution de température, les débits par évaporation et condensation et les performances globales du caloduc. Les équations elliptiques de conservation de masse, de quantité de mouvement et d'énergie jointes à la relation d'équilibre thermodynamique et aux conditions aux limites appropriées sont résolues numériquement pour un caloduc cylindrique ayant un évaporateur, un tronçon adiabatique et un condenseur. Les résultats montrent que dans certains cas les variations de pression de vapeur jouent un rôle sensible dans le fonctionnement du caloduc. On montre aussi que la solution approchée basée sur les équations paraboliques de la couche limite ne donne pas une image correcte des variations de pression de vapeur aux débits relativement grands d'évaporation et de condensation.

DER EINFLUSS DES DAMPFDRUCKABFALLS AUF DIE LEISTUNG EINES WARMEROHRES

Zusammenfassung—Es handelt sich um die Berechnung des Einflusses einer Dampdruckänderung auf die Temperaturverteilung, die Verdampfungs- und Kondensationsrate und auf die Gesamtleistung eines Wärmerohres. Did elliptischen Massen-, Impuls- und Energieerhaltungssätze in Verbindung mit der Beziehung für das thermodynamische Gleichgewicht und geeignete Randbedingungen wurden für ein zylindrisches Wärmerohr mit Verdampfungs- und Kondenstionsabschnitt- und adiabatem Zwischenstück numerisch gelöst. Die Ergebnisse zeigen, dass die Änderung des Dampfdruckes in bestimmten Situationen einen massgeblichen Einfluss auf die Leistung des Wärmerohres hat. Weiter wurde gezeigt, dass die Näherungslösung auf Grund der parabolischen Grenzschichtgleichungen kein genaues Bild von Druckänderungen bei hohen Verdampfungs- und Kondensationraten liefert.

АНАЛИЗ ВЛИЯНИЯ ПЕРЕПАДА ДАВЛЕНИЯ ПАРА НА РЕЖИМ РАБОТЫ ТЕПЛОВЫХ ТРУБ

Аннотация—Представлен анализ влияния перепада давления пара на распределение температуры пара, скорость испарения и конденсации и на режим работы тепловой трубы. Для цилиндрической тепловой трубы с испарительной, адиабатической и конденсирующей секциями численно решены эллиптические уравнения сохранения массы, количества движения и энергии вместе с соотношением термодинамического равновесия и соответствующими граничными условиями. Результаты показывают, что при определенных условиях перепад давления пара оказывает сущесгвенное влияние на режим работы тепловой трубы. Показано также, что приближенное решение, основывающееся на параболических уравнениях пограничного слоя, не дает точной картины изменения давления пара при относительно больших скоростях испарения и конденсации.